Linewidth measurement technique using through-focus optical images

Ravikiran Attota,* Richard Silver, and Ronald Dixson

Precision Engineering Division, National Institute of Standards and Technology, Gaithersburg, Maryland 20899, USA

*Corresponding author: ravikiran.attota@nist.gov

Received 2 July 2007; revised 10 December 2007; accepted 11 December 2007; posted 14 December 2007 (Doc. ID 84699); published 23 January 2008

We present a detailed experimental study of a new through-focus technique to measure critical dimension linewidth with nanometer sensitivity using a bright field optical microscope. This method relies on analyzing intensity gradients in optical images at different focus positions, here defined as the focus metric (FM) signature. The contrast of an optical image of a structured target, where a particular structure is repeated several times, varies greatly as it is moved through-focus if the spacing between the structures is such that the scattered field from the features interferes. Complex, distinguishable through-focus optical response occurs under this condition giving rise to the formation of several cyclic high and low contrast images. As a result it exhibits several FM signature peaks as opposed to a single FM peak for structures nearly isolated. This complex optical behavior is very sensitive to the dimensions of the target geometry. By appropriately analyzing the through-focus optical image, information can be obtained regarding the target. An array of lines is used as a structured target. Linewidth measurements were made by using experimental through-focus optical data obtained using a bright field microscope and simulated optical data. The optical results are compared with reference metrology tools such as a critical dimension atomic force microscope and critical dimension scanning electron microscope. © 2008 Optical Society of America

OCIS codes: 120.3940, 110.6760, 290.3700, 350.2770, 180.6900.

1. Introduction

Optical tools play a key role in semiconductor metrology because of their cost advantage and high throughput. At the same time advances in the semiconductor industry continues to result in smaller gate widths and contact holes. Optical metrology techniques are generally considered to have a disadvantage for such small targets because of the limitation due to the Raleigh criteria. However, by developing new methods of acquiring and analyzing optical data, the utility and reliability of the optical techniques as a metrology tool can be extended. For example, recently developed optical scatterometry techniques have gained widespread application to evaluate the linewidths of a grating with features much smaller than the wavelength [1]. Here we present a new technique that extends optical metrology.

The new approach presented here is applied to targets fabricated in silicon, since this is the material of choice for making semiconductor devices such as microprocessors and memory chips. The accurate measurement of these devices is extremely important to optimize device performance while minimizing production costs. As a result of the tremendous sensitivity of optical methods with the high throughput and lower relative costs of optical metrology tools, they are a particularly appealing solution to semiconductor measurement challenges, if the conventional resolution limitations can be overcome.

In conventional optical microscopy, it is usually deemed necessary to acquire images at the "best focus" position, for meaningful analysis. This is based on the belief that the most faithful representation of the target is rendered only at the best focus image. Out of focus images are ordinarily not considered particularly useful, especially for metrology applications. However, the out of focus images do contain useful information regarding the target being im-

0003-6935/08/040495-09$15.00/0

aged. The key is to use the appropriate data acquisition and analysis method. In 2004 [2] we proposed a new method, defined as the “focus metric (FM) signature” to appropriately analyze the through-focus optical images for dimensional analysis. In the same publication, based on the optical simulations, we showed the initial demonstration of high sensitivity of the FM signature method for the linewidth measurements. This method utilizes a set of through-focus optical images obtained by a conventional bright field microscope for the linewidth analysis. From 2005 onward, independent investigators successfully applied the same through-focus methodology for the linewidth measurement, primarily based on empirical analysis [3–5]. In this paper we present a comprehensive theoretical and experimental analysis based on application of the FM signature method for the linewidth measurements.

2. Focus Metric Signature

In optical microscopy it is necessary to bring a target to the best focus position repeatedly. One way to achieve this is to process the optical image as the focus is varied and evaluate a metric, which helps in focusing the target. Several methods are available to evaluate the metric [6], e.g., the Fourier transform method, the gradient energy maximization method, the high-pass filtering method, the histogram entropy method, the histogram of local variations method, the gray-level variance method, and the sum-modulus difference method. We have been using the gradient energy method for focusing [7] due to its excellent performance. In the gradient energy method, the FM is obtained by summing up the square of the intensity gradient across the field of view as the target is moved through-focus. That is,

$$\mathrm{FM} = \frac{1}{N-1}\sum_{i=2}^{N}(S_i - S_{i-1})^2,$$

where S_i is the image intensity of the ith pixel and N is the total number of pixels. The procedure we followed to calculate the FM value from an optical image using the gradient energy method is depicted in Fig. 1 for a structured target containing an array of lines. A plot of the FM value versus focus position is called the FM signature [2,8]. For features not in proximity, the FM signature usually results in a single peak, as shown in Fig. 2. The intensity profiles at various focus positions are shown in the insets for the same figure. The focus position corresponding to the maximum FM value is usually considered to be the best focus position.

The FM method is satisfactory on most targets. However, when there are several features in a target, which are close enough so that the scattered light from each feature interferes with that from neighboring features, the result is an FM signature with several peaks. We reported deviation of the FM plot from the classical single peak to multiple peaks in [2,8]. A typical example of an FM signature in this regime is

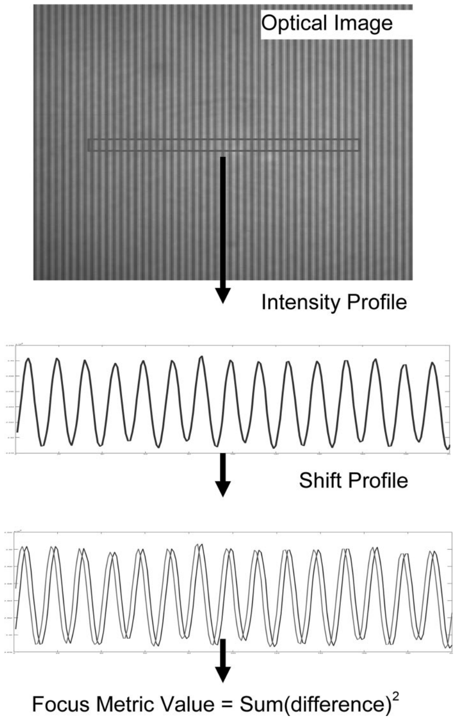

Fig. 1. Schematic showing the process of obtaining an FM value from an optical image.

shown in Fig. 3(a). Definition of the best focus position in this regime is not clear because of the presence of the two FM peaks. The figure also shows variations in the intensity profiles at different focus positions.

The following explanation can be given for the multiple peaks observed in the FM signature [9]. In Köhler illumination, each point at the back focal plane produces a plane wave of illumination at the sample plane. Each plane wave of illumination results in an independent image. Several such indepen-

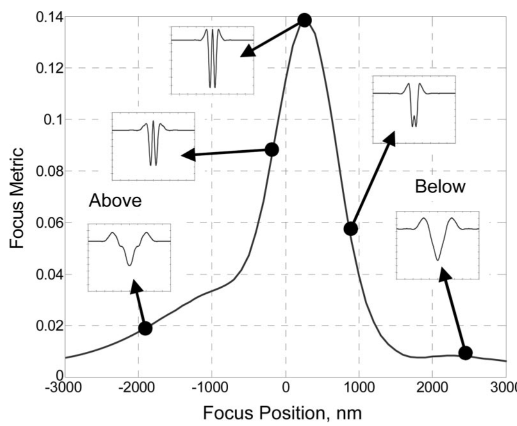

Fig. 2. FM plot obtained using a simulated profile of an array of lines, where lines are NOT optically interacting. Insets are intensity profiles at indicated focus positions. Parameters for simulation: Si line on Si substrate; linewidth = 0.5 μm, pitch = 10 μm, line height = 0.5 μm; NA = 0.8; INA = 0.4; wavelength = 546 nm. Zero position represents substrate.

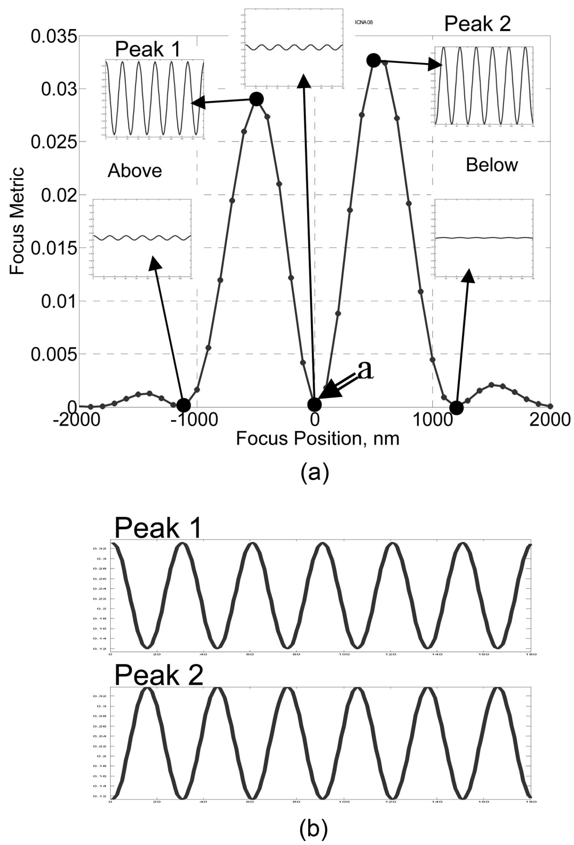

Fig. 3. (a) FM signature for the line array features exhibiting proximity effects. Insets are intensity profiles at the indicated focus positions. Parameters for simulation: linewidth = 140 nm; line height = 200 nm; pitch = 600 nm; INA = 0.4; NA = 0.8; wavelength = 546 nm. Zero position represents substrate. (b) Intensity profiles at the two FM signature peaks shown in Fig. 3(a).

dent images are formed by all the plane waves that are generated from all the points at the back focal plane. For an incoherent light source, the final image is the sum of all the individual images thus formed. In the case of a line grating target, each plane wave of illumination produces an independent image with cross-sectional intensity that has a waveform pattern. As explained before, the final image intensity is the sum of the intensity waveforms generated by all the illuminating plane waves. The intensity waveform changes with focus position. As the sample is moved through the focus, a point is reached where the intensity waveforms from the different plane waves align. Under this condition, the sum of the individual images produces a high contrast final image. Similarly, at a different focus position, the peak intensities of some waves coincide with the valley intensities of other waves (i.e., least alignment), effectively canceling out intensity variations, resulting in a very low contrast final image. As the sample is moved through the focus, depending on the experimental conditions, several such high and low contrast images form, resulting in multiple peaks in the FM signature.

Intensity profiles at the two peaks from the FM signature in Fig. 3(a) are shown in Fig. 3(b). The two profiles have a 180° intensity shift. A similar 180° shift in the intensity profiles was observed and reported by Talbot in 1836 [10]. In this early work Talbot reported that when a grating was viewed with a lens as the distance of the lens from the grating was varied, the sharpness of the grating increased and decreased several times cyclically over a large distance similar to the behavior observed in Fig. 3. A new interpretation of the Talbot effect supporting the current analysis can be found in [11,12]. In the current paper, we have presented a new related methodology using Köhler illumination, which results in a three-dimensional oscillating intensity pattern. We then harness the three-dimensional oscillating intensity pattern for metrology applications by analyzing it with the FM signature.

3. Focus Metric Signature: Sensitivity Test

The FM signature, as a result of the complex optical interactions, depends on several parameters. It depends on the target design parameters (or dimensions), such as the line pitch (P), linewidth (W), line height (H), and side wall angle (A) of an array of lines, and the optical parameters such as the collection numerical aperture (NA), illumination numerical aperture (INA), illumination wavelength (λ), and any aberrations in the optical system. We have obtained FM signatures from simulated profiles under several conditions using a "modal diffraction grating model" [13]. These results were compared with three different optical simulation models [14–16] for accuracy and were found to be in good agreement. For these simulations, we selected an Si line array on an Si substrate as the structured target, using $n = 4.1$ and $k = 0.044$ as the optical constants appropriate for a 546 nm wavelength. At present the FM signature shape appears to be unique under a given set of conditions, and hence it is referred to as a "signature." In the following paragraphs we analyze the sensitivity of the FM signature for different target and microscope parameters using the simulations.

High sensitivity to changes in the linewidth is essential for linewidth metrology applications. To study this, simulations were made for linewidths varying between 140 and 160 nm both for 5 and 1 nm variations in the linewidth. These results are presented in Fig. 4. Significant variation in the FM signature can be observed from Fig. 4(a) for 5 nm variation in the linewidth. The focus position of the FM signature peak varies considerably, that is, depending on the linewidth, each target has a different best focus position. Under these simulation conditions, a 20 nm difference in the linewidth results in an $\sim$500 nm difference in the best focus position. It is also interesting to note that the best focus position is significantly away from the top of the line. For linewidth = 160 nm, it is as far as 500 nm away from the top of the line. The FM signature shows a gradual but considerable difference for 1.0 nm changes in linewidth as shown in Fig. 4(b) indicating a good sensitivity of this method for change in the linewidths as small as 1.0 nm.

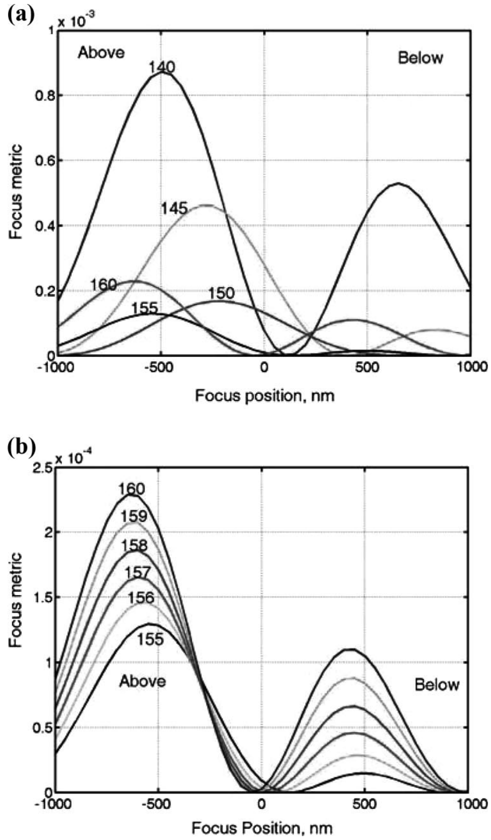

Fig. 4. FM signature obtained from the simulated profiles as a function of the linewidth in nanometers: (a) 5 nm change in the linewidth, and (b) 1 nm change in the linewidth. Pitch is 600 nm; line height is 230 nm; NA is 0.8; INA is 0.5. Zero position represents top of the line feature.

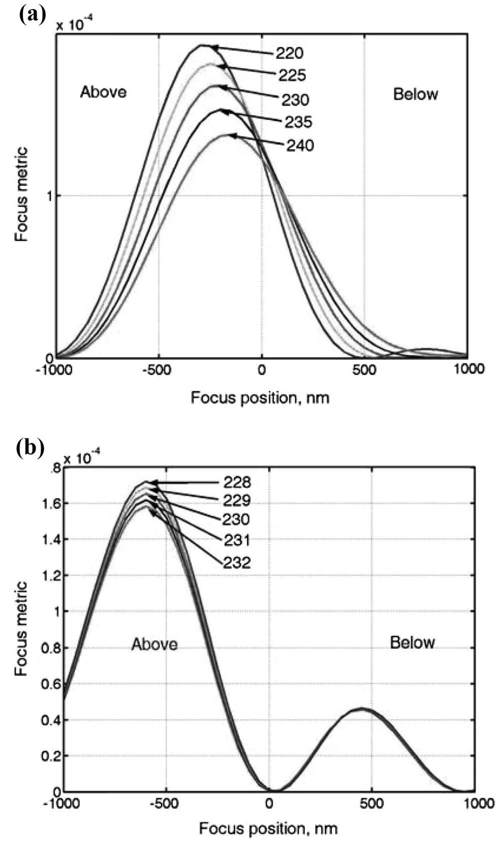

Fig. 5. FM signature obtained from the simulated profiles as a function of the line height in nanometers: (a) 5 nm change in the line height for 150 nm wide line, and (b) 1 nm change in the line height for 157 nm wide line. Pitch is 600 nm; linewidth is 150 nm; NA is 0.8; INA is 0.5. Zero position represents top of the line feature.

To apply this method to the evaluation of linewidths, it is desirable to have minimal sensitivity of the FM signature to variations in line height. For this, simulations were made for both 5 and 1 nm variations in the line height, and the results are presented in Fig. 5. Compared to linewidth, the FM signature shows less sensitivity to the line height variations. The FM signature is considerably less sensitive for a 1 nm change in the line height as shown in Fig. 5(b). High sensitivity to changes in the linewidth compared to changes in the line height is beneficial for linewidth measurements.

To estimate the sensitivity of the FM signature to small variations in the pitch, simulations were made for 5 nm changes in the pitch and are presented in Fig. 6. A small change in the pitch results in considerable change in the peak intensity. For this reason it is important to measure the pitch accurately for linewidth measurements. The positive aspect is that the pitch of a line grating is one of the most accurately measurable parameters.

Next we present the effect of microscope parameters on the FM signature. INA, which determines the maximum angle of illumination, has a dramatic influence on the FM signature as shown in Fig. 7. The number of oscillations in the FM signature increases with decreasing INA. In other words, the focus range in which oscillations in the FM signature occurs, increases with decreasing INA. This is consistent with the observation of Talbot [10], where for a plane wave illumination (i.e., close to zero INA) he reported the observation of appearing and disappearing line grating images through a focus range of several meters.

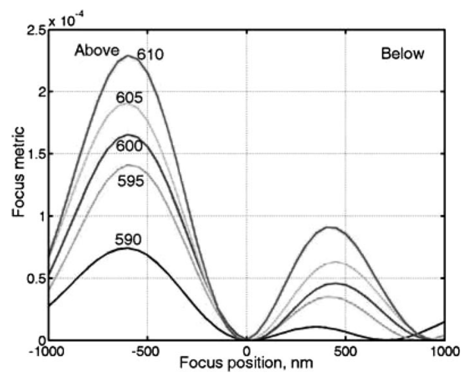

Fig. 6. FM signature obtained from simulated profiles as a function of the line pitch in nanometers. Linewidth is 157 nm; line height is 230 nm; NA is 0.8; INA is 0.5. Zero position represents top of the line feature.

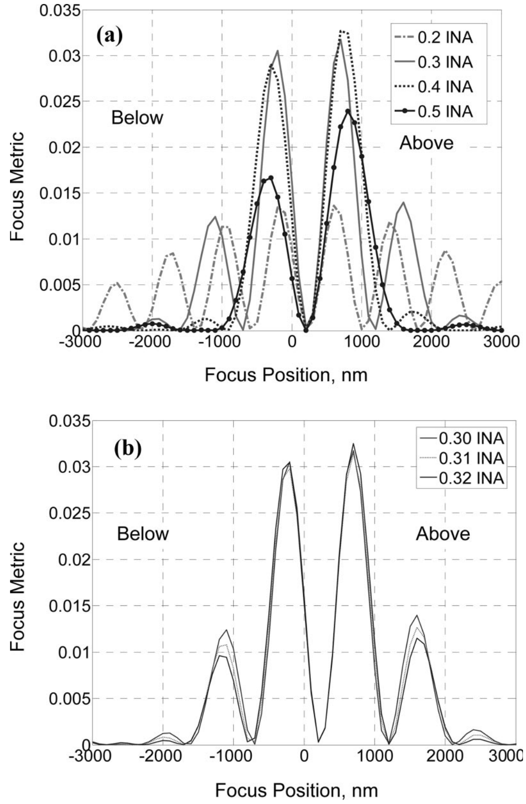

Fig. 7. FM signature as a function of the INA obtained from the simulated profiles: (a) 0.1 change in INA and (b) 0.01 change in INA. Linewidth = 140 nm; line height = 200 nm; pitch = 600 nm; NA = 0.8; wavelength = 546 nm. Zero position represents substrate.

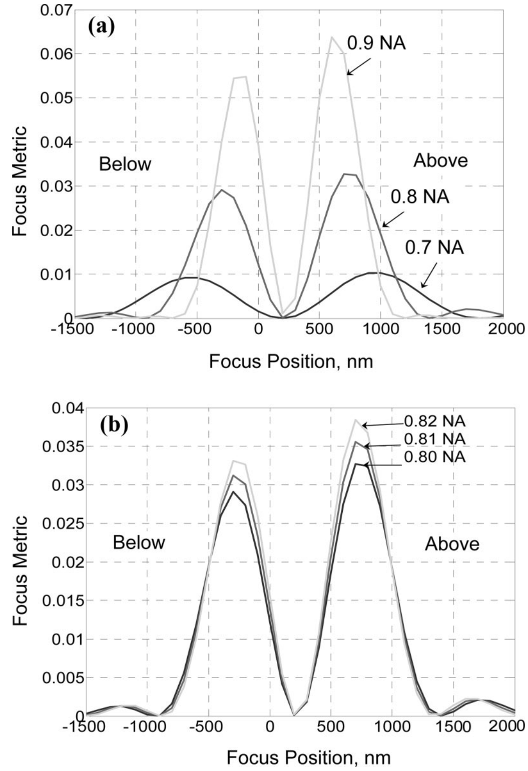

Fig. 8. FM signature as a function of the collection NA obtained from the simulated profiles: (a) 0.1 change in NA and (b) 0.01 change in NA. Linewidth = 140 nm; line height = 200 nm; pitch = 600 nm; INA = 0.4; wavelength = 546 nm. Zero position represents substrate.

The effect of a 0.01 change in INA on the FM signature is shown in Fig. 7(b). The FM signature shows sensitivity to the INA and, hence, requires accurate determination of the INA.

Simulations were performed to determine the effect of collection NA on the FM signature for typically used NA values. This determines the number of diffracted orders collected by the collection lens. A 0.1 change in the NA has considerable influence on the FM signature, as can be seen in Fig. 8(a), for a constant INA of 0.4. Figure 8(b) depicts a 0.01 change in the collection NA. It shows a measurable difference in the FM signature. As expected, sharpness of the image increases with increasing NA. Again, the best focus position changes with NA. This implies that it is essential to accurately know the NA of the optical system.

The effect of changing the illumination wavelength is shown in Fig. 9. A 10 nm change in the illumination wavelength (not including the effects of the changes in n and k, which were held fixed) results in a significant change in the FM signature [Fig. 9(a)]. However, a 1 nm change in the illumination wavelength appears to have a minor effect on the FM signature, as seen in Fig. 9(b). The three signatures almost overlap each other. Therefore a small change in the measured wavelength from the correct value may not affect the result significantly.

Figure 10 shows the importance of knowing the optical properties of the relevant materials accurately. The effect of variation in the refractive index (n) and the absorption coefficient (k) are shown in Figs. 10(a) and 10(b), respectively. The FM signature appears to be more sensitive to changes in the refractive index than changes in the absorption coefficient under the selected conditions.

The sensitivity test of various parameters presented above is not an exhaustive study. Under a given set of conditions some parameters will be more sensitive than others, while under a different set of conditions other parameters may be more sensitive. Based upon the sensitivity results presented above from the simulations, the following observations can be made. The FM signature appears to be more sensitive to changes in the linewidth compared to changes in the line height. It is a challenge to accurately measure linewidth. However, it is trivial to obtain the line height with good accuracy using an atomic force microscope. INA and collection NA appear to have a similar effect on the FM signature. However, with some effort it is possible to measure both of these values reasonably accurately. Small variations in the illumination wavelength appear to have a minor influence on the FM signature. The refractive index has a stronger influence on the FM signature compared to the absorption coefficient. The sensitivity on both the illumination and collection

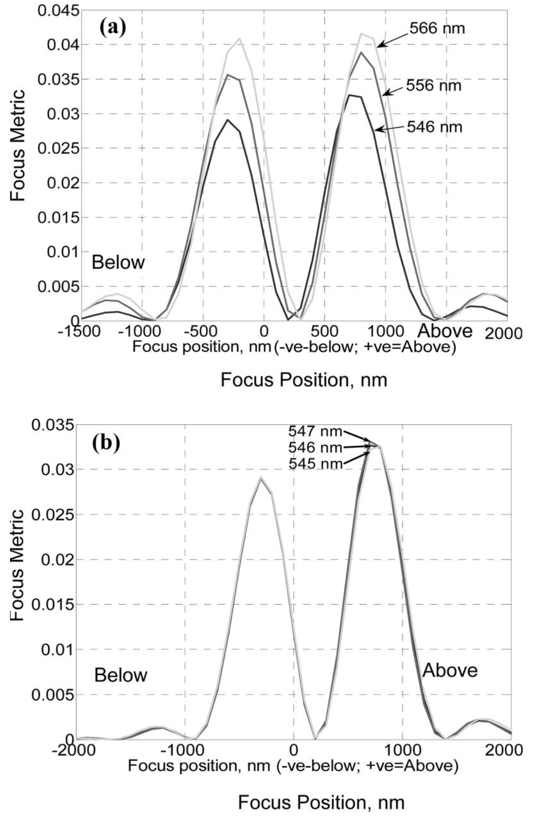

Fig. 9. FM signature as a function of the illumination wavelength obtained from the simulated profiles: (a) 10 nm change in the wavelength and (b) 1 nm change in the wavelength. Linewidth = 140 nm; line height = 200 nm; pitch = 600 nm; INA = 0.4; NA = 0.8. Zero position represents substrate.

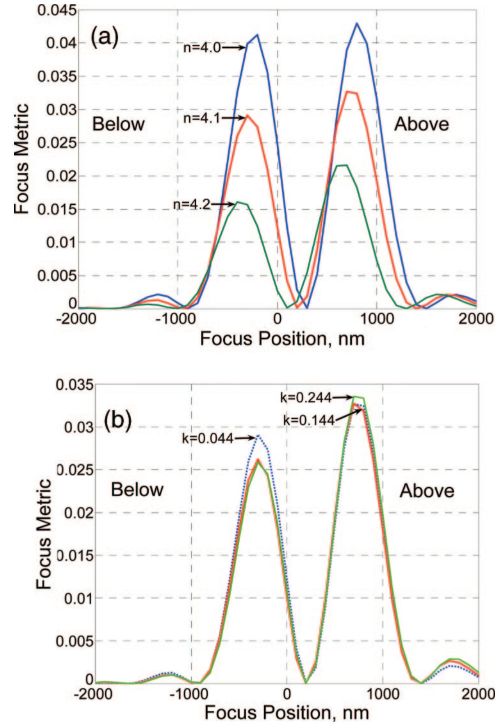

Fig. 10. (Color online) FM signature as a function of the optical properties obtained from the simulated profiles: (a) 0.1 nm change in the refractive index (n) and (b) 0.1 nm change in the absorption coefficient (k). Linewidth = 140 nm; line height = 200 nm; pitch = 600 nm; NA = 0.4; NA = 0.8. Zero position represents substrate.

NAs suggests that, for quantitative measurements, accurate values of both the NAs are required. Based on the understanding gained with the simulated results, an attempt has been made to experimentally measure the linewidth using a bright field optical microscope in Section 4.

4. Evaluation of the Linewidth Using the Focus Metric Signature

A. Focus Metric Signature Experiments

Experimental evaluation of the linewidth is presented in this subsection. An etched Si wafer, where each die was exposed slightly differently resulting in a small variation in the linewidths, was used for this study. A 100 μm $\times$ 100 μm scatterometry target with a designed nominal linewidth of 100 nm and a pitch of 600 nm was selected for the linewidth analysis. The linewidths and pitches of the targets in several die were measured using a calibrated critical dimension-scanning electron microscope (CD-SEM) and a calibrated critical dimension atomic force microscope (CD-AFM). From these results, a selection of die with small variation in the bottom linewidth were identified for further analysis. The line height and the sidewall shape were obtained using a CD-AFM. These values are presented in Fig. 11.

The selected targets were imaged through the focus in 100 nm step size increments using an optical microscope with 0.8 collection NA, 0.39 INA, 546 nm illumination wavelength, and 50$\times$ objective magnification. Each experiment was repeated at least three times. The mean, normalized experimental FM signatures are presented in Fig. 12 along with the measured CD-SEM values and their standard deviations. This shows good experimental sensitivity to nanometer changes in linewidth using the FM signature method.

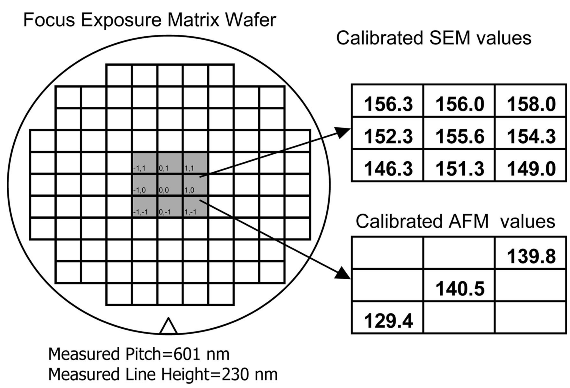

Fig. 11. Measured bottom linewidth values in nanometers, using CD-SEM and CD-AFM.

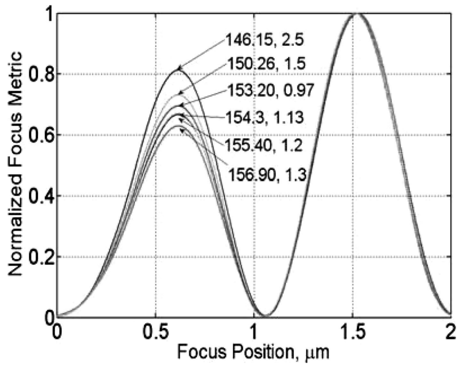

Fig. 12. Mean experimental FM signatures for the six target locations selected normalized to the bigger FM peak. The SEM measured linewidths and their standard deviations are indicated in the figure in nanometers.

B. Focus Metric Signature Experiments and the Simulations Comparison

A critical element of the experiment to simulation comparisons is accurate knowledge of the experimental conditions so as to perform simulations with the correct input parameters. The needed input parameters for the simulations can be divided into two broad categories: (1) target related parameters and (2) microscope related parameters. The required target related input parameters are starting point linewidth values, height, pitch, sidewall shape, and optical properties. Except for the linewidth, all of the input parameters can be reasonably well characterized using the appropriate instrumentation. The microscope related input parameters needed are INA, collection NA, illumination wavelength, and illumination homogeneity. The microscope used in the work presented in this subsection had reasonably good illumination homogeneity [9]. The other measured microscope parameters are presented in Subsection 4.A. However, the INA needs some further explanation.

An alternative method to infer the INA by comparing the simulated and the experimental FM signatures was presented in a previous publication [17]. The FM signatures have proven to be very sensitive to the INA. Since the FM signatures depend on the INA, it can be evaluated experimentally, provided all the other input parameters are well characterized and known. In [17], using a traditional geometrical method, where the largest angle of illumination is measured, the measured INA was found to be nominally 0.50. However, the effective INA measured by matching the experimental FM signature with the simulated FM signature was 0.42. Subsequent to the study presented here, a major cause of this effective lower INA on the tool used in this work was identified as significant differences in the intensity transmission of the "*s*" and "*p*" polarized light at larger incident angles. For more information on this, refer to Silver *et al.* [18].

The measured INA of the microscope used in the current study using the standard geometrical approach is 0.39. Based on the discussion in the preceding paragraph, it is likely that the effective INA of the microscope is less than 0.39. However, the exact effective lower INA is not known. As a result, two unknowns need to be evaluated: the linewidth and the INA. Based on the prior knowledge of the approximate values for both the linewidth and the INA, parametric analysis with two floating parameters was performed in an attempt to evaluate the linewidths.

The measured CD-SEM and CD-AFM values have approximately 15 nm offset with respect to one another (Fig. 11). However, the die-to-die differences in the CD values are nearly the same for the two methods, indicating that both methods have good linearity and sensitivity. The accuracy of the CD-SEM measurements is dependent upon the edge-detection algorithms used in the SEM and the particular geometry of these features. Consequently, the uncertainty of the SEM measurements was not thoroughly characterized for these measurements. The accuracy of the CD-AFM measurements themselves is better understood, but there are also measure and definition uncertainties to consider when comparing the optical, SEM, and AFM results.

Recent National Institute of Standards and Technology (NIST) work in CD-AFM reference metrology has led to the capability to calibrate the CD-AFM tip width with a standard uncertainty ($k = 1$) as low as 0.8 nm [19,20]. This means that for the linewidth measurement of near vertical structures, the standard uncertainty of CD-AFM measurements can approach the level of 1 nm. However, in addition to the tip width calibration uncertainty, there are also "higher order" or shape-related tip effects that can be significant for measurements on less idealized structures, especially those with nonvertical sidewalls [21].

The features measured in this paper are particularly challenging for AFM, since the feature sidewalls have realistic nonvertical sidewalls and exhibit a significant deviation from vertical, and the cross-sectional profiles are also not well described by a trapezoidal model. This limits the reliability of any attempt to extrapolate the AFM results to the very base of the structure, where the tip does not contact the surface. The standard uncertainties of the AFM values themselves are estimated to be ~4 nm, including contributions from tip calibration and tip wear, but this uncertainty estimate applies only to the width that the AFM actually "sees." For the particular tip used in this work, the bottom 25 nm of the structure was not contacted by the flare of the tip. Although we performed an extrapolation to estimate the width of the structure at the base—which was necessary to compare with the SEM and optical results—the uncertainty in this extrapolation is not well defined. For structures that are close to trapezoidal, this uncertainty can be reasonably estimated, but the issue of possible "footing" at the base of the structure always remains a concern.

Using the available input parameters, the FM signatures were obtained by simulation for linewidths varying from 125 to 175 nm and INAs varying from

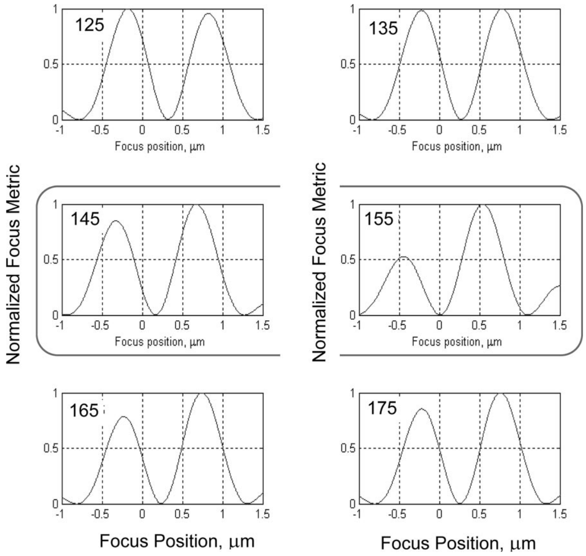

Fig. 13. Simulated FM signatures for 125, 135, 145, 155, 165, and 175 nm bottom linewidths at 0.37 INA. Other input parameters are: line height = 230 nm, pitch = 601 nm, collection NA = 0.8, illumination wavelength = 546 nm, and Si lines on Si substrate.

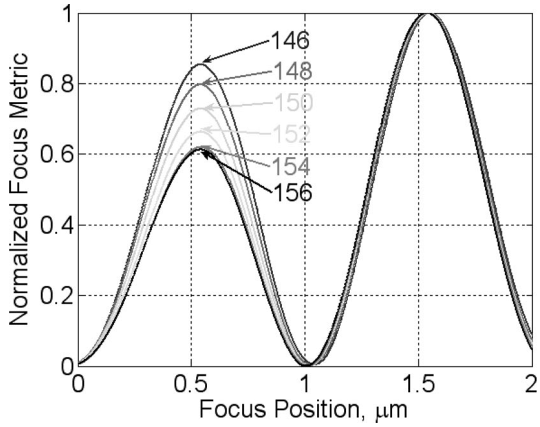

Fig. 14. Simulated FM signatures for 146 to 156 nm bottom linewidths at 0.36 INA. Other input parameters are: line height = 230 nm, pitch = 601 nm, collection NA = 0.8, wavelength = 546 nm, and Si lines on Si substrate.

0.35 to 0.39. For the range of INAs modeled, qualitative agreement between the simulated FM signatures for 125 and 135 nm linewidths and the experimental FM signatures (see Figs. 12 and 13) is not achieved. However, qualitative agreement between the simulated FM signatures (see Fig. 13) and the experimental profiles is obtained for the linewidths in the range of 145, 155, 165, and 175 nm. The match between the simulations and the experimental results is optimized with a choice of INA of 0.37, which is a reasonable choice based on the effective NA discussion above. A closer look at the experimental FM signatures show that the left peak FM value decreases with increasing linewidth. A decreasing left peak FM value is only observed for the linewidth simulations between 135 and 155 nm. For the linewidths between 155 and 175 nm, the left peak FM value increases. Therefore, this analysis indicates that the experimental targets measured here have linewidths between 140 and 155 nm.

To perform a more detailed analysis in this range, the simulated optical FM signatures were obtained at 2 nm linewidth increments from 146 to 156 nm and for INAs varying between 0.35 and 0.39. Comparison of the difference between the experimental left intensity peaks with simulated left intensity peaks for a 10 nm range of linewidths showed that the 0.36 INA data matched closest to the experimental data. This test indicated that the effective INA is in fact closest to the 0.36 value. The simulated FM signatures for 0.36 INA are presented in Fig. 14 and show good qualitative agreement with the experimental FM signatures in Fig. 12.

Based on the analysis of the simulated and the experimental FM signatures, we evaluated the linewidth values for the targets selected. Figure 15 shows the normalized left peak FM value as a function of linewidth for both the simulations and the experiments. The curve in the figure labeled simulation is a plot of the simulated left peak FM values versus the linewidth values used as inputs to the simulations. The curve labeled experimental is a plot of the experimental left peak FM values versus the SEM measured linewidth values. By matching the intensity of the experimental FM value with the simulated FM value, linewidths for all of the selected targets were evaluated based exclusively on modeled results without reference to the SEM data as seen in Fig. 16. In this initial attempt to quantitatively measure linewidths with the FM signature method based exclusively on the optical techniques, a good qualitative agreement was observed between the SEM, AFM, and the optical FM signature methods.

Although the methods presented here were applied to silicon linewidth measurement, the methods are more general and may be applied to a variety of targets and materials. The principal requirement is that the target be periodic, having at least several periods, and that the pitch or line spacing be large enough to ensure that higher order optical diffraction content is captured by the optical tool. In addition, the through-focus methodology can be applied to two-dimensional arrays.

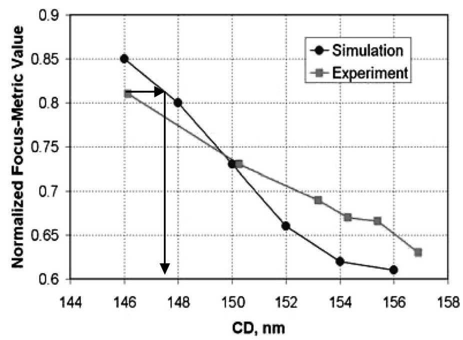

Fig. 15. Plot of the normalized left peak intensity versus the linewidth for the simulations and the experiments.

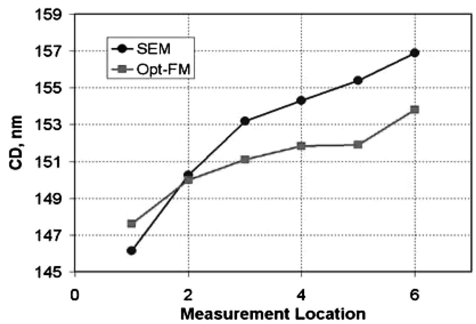

Fig. 16. Measured linewidths using the SEM and the FM signature optical microscope method.

5. Summary

In this paper we have presented a new method for evaluating the linewidth of a grating using a bright field optical microscope. The gradient energy FM signature method was used to analyze the optical response of the target as it is moved through-focus in an optical microscope to obtain the FM signature. A line grating with features in close proximity produces several oscillating cycles in the FM signature. Using the optical simulations we demonstrated that the FM signature is sensitive to (a) the target related parameters such as the linewidth, pitch, height, and optical properties of the material and (b) the optical parameters such as the INA, collection NA, and wavelength of the illumination. The optical simulation results strongly point to the uniqueness of the FM signature under a given set of the experimental conditions. By comparing the experimental FM signatures with that of the simulated FM signatures we have successively evaluated quantitative linewidth (critical dimension) measurements exclusively using the optical techniques. The results using the optical methods showed good qualitative agreement with both the CD-AFM and the CD-SEM measurements.

The authors thank the Office of Microelectronics Programs of NIST for financial support and Semiconductor Manufacturing Technology (SEMATECH) for wafer fabrication support. The authors also thank Robert Larrabee, James Potzick, Thomas Germer, Michael Stocker, Heather Patrick, Bryan Barnes, Egon Marx, and Mark Davidson for assistance and useful discussions.

References

1. C. J. Raymond, S. S. H. Naqvi, and J. R. McNeil, “Scatterometry for CD measurements of etched structures,” Proc. SPIE **2725,** 720–728 (1996).
2. R. Attota, R. M. Silver, M. Bishop, E. Marx, J. Jun, M. Stocker, M. Davidson, and R. Larrabee, “Evaluation of new in-chip and arrayed line overlay target designs,” Proc. SPIE **5375,** 395–402 (2004).
3. Y.-S. Ku, A.-S. Liu, and N. Smith, “Through-focus technique for nano-scale grating pitch and linewidth analysis,” Opt. Express **13,** 6699–6708 (2005).
4. A.-S. Liu, Y.-S. Ku, and N. Smith, “Through-focus algorithm to improve overlay tool performance,” Proc. SPIE **5908,** 383–391 (2005).
5. Y.-S. Ku, A.-S. Liu, and N. Smith, “Through-focus technique for grating linewidth analysis with nanometer sensitivity,” Opt. Eng. **45,** 123602 (2006).
6. E. Krotkov, “Focusing,” Int. J. Comput. Vis. **1,** 223–237 (1987).
7. S. Fox, R. M. Silver, E. Kornegay, and M. Dagenais, “Focus and edge detection algorithms and their relevance to the development of an optical overlay calibration standard,” Proc. SPIE **3677,** 95–106 (1999).
8. R. M. Silver, R. Attota, M. Stocker, M. Bishop, J. Jun, E. Marx, M. Davidson, and R. Larrabee, “High resolution optical overlay metrology,” Proc. SPIE **5375,** 78–95 (2004).
9. R. Attota, R. M. Silver, and J. Potzick, “Optical illumination and critical dimension analysis using the through-focus focus metric,” Proc. SPIE **6289,** 62890Q (2006).
10. H. F. Talbot, “Facts relating to optical science, No. IV,” Philos. Mag. **9,** 401–407 (1836).
11. P. Latimer and R. F. Crouse, “Talbot effect reinterpreted,” Appl. Opt. **31,** 80–89 (1992).
12. P. Latimer, “Talbot plane patterns: grating images or interference effects?,” Appl. Opt. **32,** 1078–1083 (1993).
13. M. Davidson, “Analytic waveguide solutions and the coherence probe microscope,” Microelectron. Eng. **13,** 523–526 (1991).
14. E. Marx, “Images of strips on and trenches in substrates,” Appl. Opt. **46,** 5571–5587 (2007).
15. T. A. Germer and E. Marx, “Simulations of optical microscope images,” Proc. SPIE **6152,** 61520I (2006).
16. T. V. Pistor, “Electromagnetic simulation and modeling with applications in lithography,” Ph.D. dissertation (University of California at Berkeley, 2001).
17. R. Attota, R. M. Silver, T. A. Germer, M. Bishop, R. Larrabee, M. T. Stocker, and L. Howard, “Application of through-focus focus-metric analysis in high resolution optical metrology,” Proc. SPIE **5752,** 1441–1449 (2005).
18. R. M. Silver, B. M. Barnes, R. Attota, J. Jun, J. Filliben, J. Soto, M. Stocker, P. Lipscomb, E. Marx, H. J. Patrick, R. Dixson, and R. Larrabee, “The limits of image-based optical metrology,” Proc. SPIE **6152,** 61520Z (2006).
19. R. G. Dixson, R. A. Allen, W. F. Guthrie, and M. W. Cresswell, “Traceable calibration of critical-dimension atomic force microscope linewidth measurements with nanometer uncertainty,” J. Vac. Sci. Technol. B **23,** 3028–3032 (2005).
20. N. Orji, A. Martinez, R. Dixson, and J. Allgair, “Progress on implementation of a CD–AFM based reference measurement system,” Proc. SPIE **6152,** 61520O (2006).
21. N. G. Orji and R. G. Dixson, “Higher order tip effects in traceable CD-AFM based linewidth measurements,” Meas. Sci. and Technol. **18,** 448–455 (2007).